

# The Role of Heterogeneous Environment and Docetaxel Gradient in the Emergence of Polyploid, Mesenchymal and Resistant Prostate Cancer Cells

Ke-Chih Lin<sup>1\*</sup>, Gonzalo Torga<sup>2\*</sup>, Yusha Sun<sup>1</sup>, Robert Axelrod<sup>3</sup>, Kenneth J. Pienta<sup>2</sup>, James C. Sturm<sup>1</sup>, Robert H. Austin<sup>1</sup>

## Abstract

The ability of a population of PC3 prostate epithelial cancer cells to become resistant to docetaxel therapy and progress to a mesenchymal state remains a fundamental problem. The progression towards resistance is difficult to directly study in heterogeneous ecological environments such as tumors. In this work, we use a micro-fabricated “evolution accelerator” environment to create a complex heterogeneous yet controllable in-vitro environment with a spatially-varying drug concentration. With such a structure we observe the rapid emergence of a surprisingly large number of polyploid giant cancer cells (PGCCs) in regions of very high drug concentration, which does not occur in conventional cell culture of uniform concentration. This emergence of PGCCs in a high drug environment is due to migration of diploid epithelial cells from regions of low drug concentration, where they proliferate, to regions of high drug concentration, where they rapidly convert to PGCCs. Such a mechanism can only occur in spatially-varying rather than homogeneous environments. Further, PGCCs exhibit increased expression of the mesenchymal marker ZEB1 in the same high-drug regions where they are formed, suggesting the possible induction of an epithelial to mesenchymal transition (EMT) in these cells. This is consistent with prior work suggesting the PGCC cells are mediators of resistance in response to chemotherapeutic stress. Taken together, this work shows the key role of spatial heterogeneity and the migration of proliferative diploid cells to form PGCCs as a survival strategy for the cancer population, with implications for new therapies.

## Keywords

Polyploid Giant Cancer Cells. Cancer-on-a-chip. Tumor microenvironment. Chemotherapy gradient. Cell migration. Metastasis.

## Abbreviations

PGCC: polyploid giant cancer cell  
EA: Evolution Accelerator  
IF: immunofluorescence  
ZEB1: Zinc finger E-box-binding homeobox 1

<sup>1</sup>Princeton University, Princeton, NJ, USA.

<sup>2</sup>Johns Hopkins Medical Institute, Baltimore, MD, USA.

<sup>3</sup>University of Michigan, Ann Arbor, MI, USA.

\* Co-lead Authors

## Contact Information

Ke-Chih Lin	(corresponding author) kechihl@princeton.edu
Gonzalo Torga	gtorga@jhmi.edu
Yusha Sun	yysun@princeton.edu
Robert Axelrod	axe@umich.edu
Kenneth J. Pienta	kpienta1@jhmi.edu
James C. Sturm	sturm@princeton.edu
Robert H. Austin	austin@princeton.edu

## 1. Introduction

Clinical studies have shown that polyploid giant cancer cells (PGCCs), morphologically-distinct cancer cells commonly observed in tumor biopsies [1], correlate with poor response to docetaxel chemotherapy in the context of castration-resistant prostate cancer [2]. PGCCs are typically multi-nucleated or have an enlarged nucleus containing multiple sets of chromosomes in comparison to most of the cells comprising the bulk of the tumor. There are multiple ways PGCCs can form: PGCCs can emerge from what would seem to be dead-end loss of function events such as abrogated mitotic checkpoint, cell fusion [3], failed cytokinesis [4], and DNA endoredu-

plication [5]. Particularly, fusion between cancer cells and normal cells, or among cancer cells themselves, has also been suspected to contribute to phenotypic evolution during different stages of cancer progression and metastasis [6]. It has been demonstrated that dual metastasis organotropisms can be achieved in the same cell through spontaneous fusion between bone- and lung-tropic sublines of the MDA-MB-231 breast cancer cell line. [7] However, PGCCs have also been observed to emerge from high-stress environments such as severe genotoxic stress (gamma irradiation [8, 3]), chemotherapy treatment (e.g. bleomycin [5], docetaxel [9, 10], cisplatin [11]), and hypoxia conditions [12, 13, 14], revealing a more important role for PGCCs. Furthermore, there is evidence that these PGCCs possess tumorigenic potential: both the mitotic-catastrophe-evaded PGCCs and the progeny derived from PGCCs may have an increased survival advantage [2].

Therefore, it is important to understand the conditions that lead to the emergence of PGCCs with chemotherapy [15]. *In vivo* animal models have proved difficult to control systematically. However, most *in vitro* cancer cell studies are either done in a well-mixed conventional cell culture setting with uniform drug concentrations which do not replicate the true complexity of *in vivo* tumors or from spheroids which are difficult to image at the single cell level. The true dynamics of PGCC emergence from an ecological perspective under stress remain unobserved in the context of the highly complex heterogeneity of the tumor ecosystem.

In a recent paper we presented an engineered microenvironment and cell culturing platform, the Evolution Accelerator (EA) [16], which allows the quantitative study of both the interactions of multiple cell types and their movement on a spatially-varying chemotherapy concentration landscape over a period of several weeks. We now show using our technology, in combination with engineered nuclear fluorescence markers, that the survivor cells at high docetaxel concentrations are in fact PGCCs. Further, we consider the main contribution of this paper to be that very large numbers of PGCCs are formed in higher drug regions in our culture, and that result from chemotherapy stress gradient (spatially-varying docetaxel concentration) and diploid cell population migration to high drug region. The elevated PGCC emergence and the increased survival of the entire cancer population directly depend on the heterogeneous environment.

Our EA technology (Fig. 1) provides a platform to investigate the emergence of PGCCs and their population dynamics in a chemotherapy induced stress landscape due to the following features:

- Fresh media with desired concentration of drug is continuously provided by syringe pump, which secures a predetermined maximal dosage and establishes stable drug gradient via cross diffusion (Fig. 1 (A)).
- Cells are partially confined within hexagonal wells called microhabitats, but they can move from microhabitat to microhabitat through channels (Fig. 1 (B)).

- The system allows real-time monitoring at single-cell level in bright field and fluorescent channels.
- The system allows for spatially resolved downstream immunofluorescence (IF) assays and direct sampling removal of cells for further characterization.
- Our experiments are carried out over multiple weeks, with constant data collection. This observation of the emergence of phenotypes that would not be observed in short time experiments.
- The EA technology of semi-isolated populations in a gradient environment accelerates evolutionary dynamics to take place over weeks in the lab rather than months in conventional *in vitro* assays.

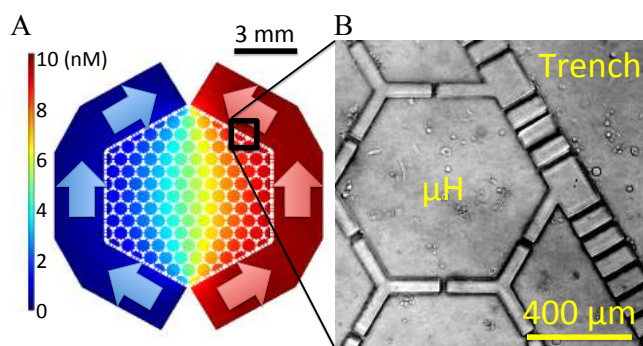


**Figure 1. The distribution of the chemical concentration in EA.** (A) The COMSOL Multiphysics<sup>®</sup> modeling of reagent concentration pattern. The diffusion coefficient is  $10^{-9} m^2/s$  and the boundary condition at the peripheral media trenches is set as 0 and 10 nM. Media flow rate is  $20 \mu L/hr$ . The reagent diffuses into the microhabitat array from the right three edges and out from the left. (B) A bright field image of the chip. Small slits ( $15 \mu m$  wide) restrict the direct media flow from the trenches into the microhabitat array. Large slits ( $25 \mu m$  wide) allow cell migration between adjacent habitats.

The technology presented here can with single-cell resolution measure the movement and ploidy status of cancer cells over a drug gradient. Lethality usually requires the gain of the metastatic phenotype, which enables cancer cells to emigrate from the primary tumor and colonize secondary sites progressing to lethal metastatic disease. This migratory phenotype has been widely associated with the epithelial-mesenchymal transition [17].

We chose a monomorphic sub-line epithelial phenotype of a widely established human prostate cancer cell to lower the intrinsic heterogeneity in the initial cancer population and highlight the emergence of the mesenchymal phenotype under chemotherapy stress. The sub-line we chose is the epithelial prostate cancer sub-line PC3-Epi, an E-cadherin/CDH1-positive-vimentin-negative PC3 derivative described by Roca *et al.* [18]. PC3-Epi cells were genetically engineered with nuclear fluorescence markers to visualize chromatin. The

mCherry-expressing PC3-Epi cell line was transfected with a H2B-GFP plasmid delivered by transfection reagent lipofectamine 2000 and selected with neomycin (G418). The H2B-GFP plasmid (Addgene plasmid # 11680) allows high-resolution imaging of chromatin without affecting cell cycle progression or the chromosomal architecture [19] Utilizing this H2B-GFP system, we are able to quantify the number of nuclei and area at the single-cell level, allowing us to study the dynamics in the emergence of polyploidy as a function of time and variable stress level across the EA ecology.

## 2. Results

There are two important results: 1) A drug gradient vastly increases the emergence of PGCCs at higher levels of docetaxel concentration and improves overall survival of cancer population, a phenomenon that cannot be understood using fixed drug concentrations in conventional static culture. 2) By downstream immunofluorescent analysis, the PGCCs emerging at the highest docetaxel concentrations in a gradient landscape show higher expression levels of ZEB1, a mesenchymal biomarker that is associated with cancer invasiveness and metastatic potential.

The PC3-Epi cells were seeded uniformly before the application of the drug in all the experiments. Cells were seeded and incubated 12 hours before the installation of the PDMS microfluidic device by placing the array over the cells on the Lumox surface and pressurizing at 0.1 bar pressure from below with 5% CO<sub>2</sub> conditioned gas under normoxia conditions. Media with no drug flow was injected through the left 3 sides of the hexagonal array of the EA while media with drug flow was injected through the right 3 sides of the hexagonal array of EA (Fig. 1 (A)). After the establishment of a docetaxel gradient over a 24-hour period (defined as  $t = 0$ ), time lapse video-microscopy scanning was performed every 30 minutes throughout the experiment to capture the dynamics of each individual cell in the array of the EA. After 17 days of cell culture, the microfluidic array was detached from the Lumox film and cells adhered to the Lumox were fixed and permeabilized for downstream immunofluorescent (IF) analysis as discussed below (Section 2.2).

Two control experiments were performed to examine the relevance of gradients and sequestered microhabitats: 1) A series of fixed drug concentrations in a series of conventional cell culture. These control experiments were performed in triplicate with the same PC3-Epi sub-cell line but seeded into a multiple-well plate with fixed docetaxel concentrations from 0 to 10 nM. The media was replenished on a daily basis in each well to maintain constant nutrients level and docetaxel concentration. 2) The EA experiment was repeated, but with single uniform drug concentration across the EA landscape (not spatially-varying). This was to check if there were some unusual feature of the EA experimental environment compared to conventional static cell cultures (besides the concentration gradient in the EA experiment described above).

### 2.1 Increased PGCCs formation and enhanced docetaxel tolerance in a gradient

A docetaxel gradient ranging from 0 to 5 nM was established across the EA. Time-lapse video-microscopy using large-area image stitching was done throughout the span of the experiment. The concentration of docetaxel in each EA microhabitat was determined by COMSOL Multiphysics<sup>®</sup> simulation. Fig. 2 presents the progression of the PC3-Epi cells in the EA versus time. We developed a custom image processing macro on ImageJ to track and pseudo-colorize the cells by mean diameter. Further details are described in the Methods section. Cells pseudo-colored green have diameters greater than 80  $\mu\text{m}$ ; smaller cells are pseudo-colored red. The detection accuracy ranges from 75% to 90% depending on cell confluence. Before the application of chemotherapy, the number of cells in each microhabitat was relatively uniform. The average cell size was also identical across the device. After 250 hours of chemotherapy treatment, cells gradually died out around the edges with the highest dosage of docetaxel. However, there were still some extremely large cells that appeared and survived within the extreme environment at the high dosage areas. The distinct cell morphology and increased ploidy confirm the emerging large cells as PGCCs.

We now look inside the EA in detail and quantify cell populations as a function of the local drug concentration. PGCC PC3 cells have been previously described to emerge when cultured in the presence of docetaxel in conventional culture [2]. Our results show that the number of PGCCs depends strongly on the existence of a gradient and not just the local value of the drug concentration. An EA experiment was performed with 0-10 nM docetaxel to fully cover the cytotoxic response range of PC3-EPI cells. The growth of PC3-EPI cells in conventional single wells and in the EA is compared in Fig. 3 (A) (B). At the left edges of the EA where the drug concentration is 0 nM the cells reached and maintained 100% confluence. In regions of increasing docetaxel concentrations, the cell confluence was basically unchanged until a steep drop was observed from 3 to 6 nM. In the single-well control experiment by the 10<sup>th</sup> day, the cell confluence decreased significantly at lower docetaxel concentrations of 2 nM.

To better visualize cell viability across docetaxel concentrations under both scenarios, the total cell confluence on the 10th day at different docetaxel concentrations is shown in Fig. 4 (A). Within each subpopulation, the density of PGCCs was quantified (Fig. 4 (B)), and the corresponding fractional population of PGCCs is shown in Fig. 4 (C).

As shown in Fig. 4 (A), the overall cell population boundary shifted positively for about 2 nM when the drug gradient was presented. The cell confluence profile of the EA gradient experiment shifted towards higher drug concentrations compared with control experiment - the population remained fully confluent until around 2 nM.

Compared with the control experiment, where the cells were cultured in conventional single-well with no docetaxel gradient, a striking result with respect to PGCCs was observed.

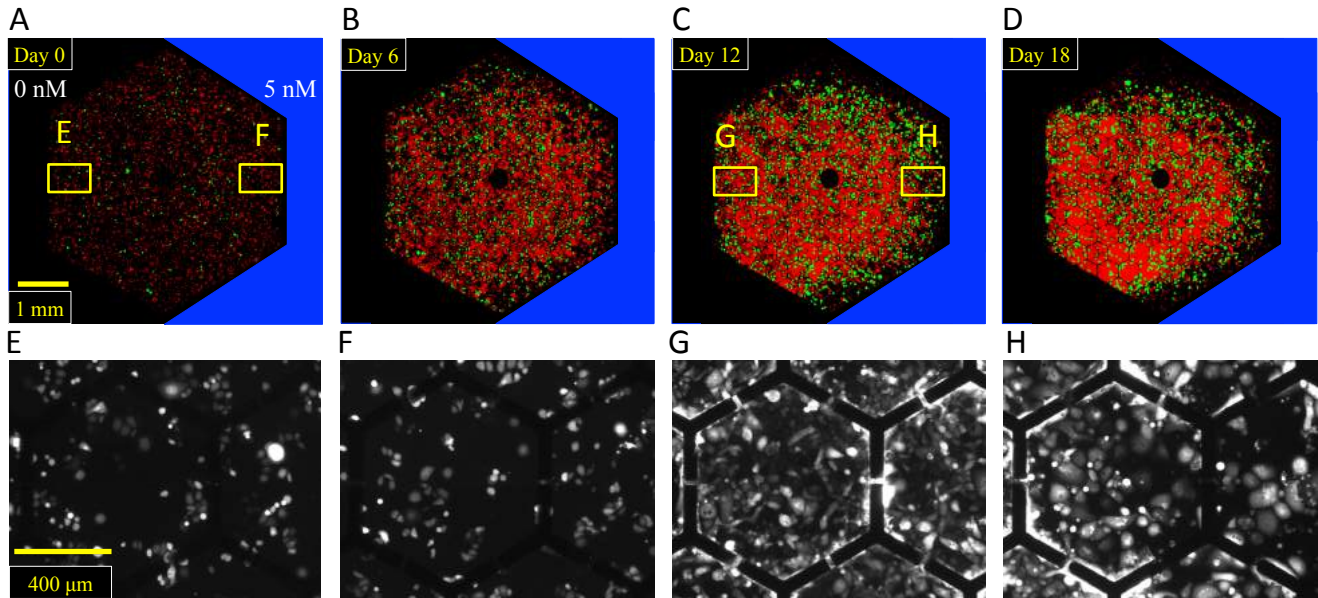


**Figure 2. PC3-EPI cultured in the EA in stress gradients (spatially-varying docetaxel concentration) (from 0 to 5 nM) for 18 days.** Cells below  $80 \mu\text{m}$  diameter are colored red and cells with diameter above  $80 \mu\text{m}$  are colored green. Regions E and F at the 0 and 5 nM drug gradient at  $t=0$  respectively are expanded, as are regions G and H at  $t=12$  days. Note that at  $t=0$ , cells at low and high dosage region E and F had similar morphology and cell size, while at  $t=12$ , cells at high dosage region H had significantly larger size compared with cells at low dosage region G.

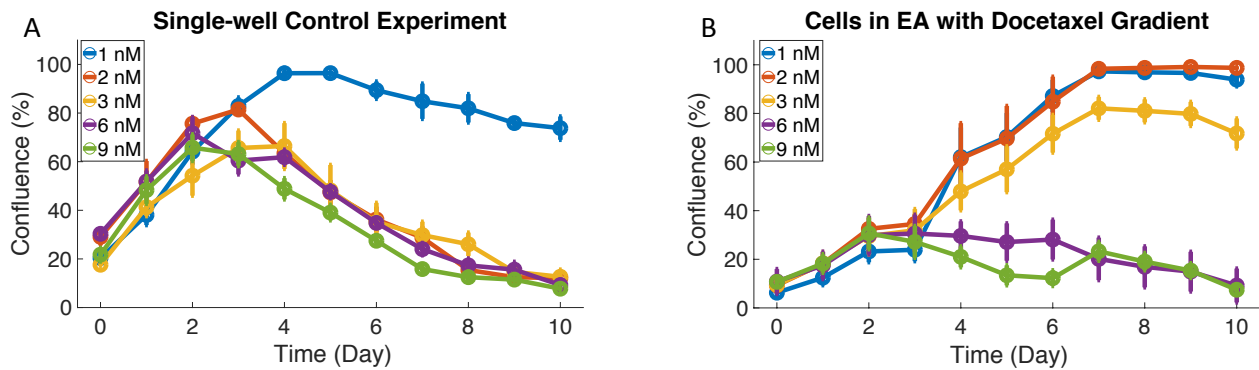


**Figure 3. The population dynamics of PC3 and PGCCs in the EA and isolated wells.** (A) PC3-EPI cells were cultured in conventional single-well plates with different docetaxel concentrations. Growth media was replenished on a daily basis with assigned dosage of drug to maintain constant nutrients level and docetaxel concentration. The growth curves show the progression of PC3-EPI in terms of confluence in a well-mixed environment. (B) PC3-EPI were cultured in the presented microfluidic EA device with docetaxel gradient (0 to 10 nM). The progression of PC3-EPI was quantified by measuring the confluence of cells in each microhabitats as a function of time. Each microhabitat corresponds to a drug concentration determined by COMSOL Multiphysics<sup>®</sup> simulation. Note in single-well control, cell confluence dropped drastically at 2 nM docetaxel and higher dosage, while in EA experiment, cells remained highly confluent at 3 nM.



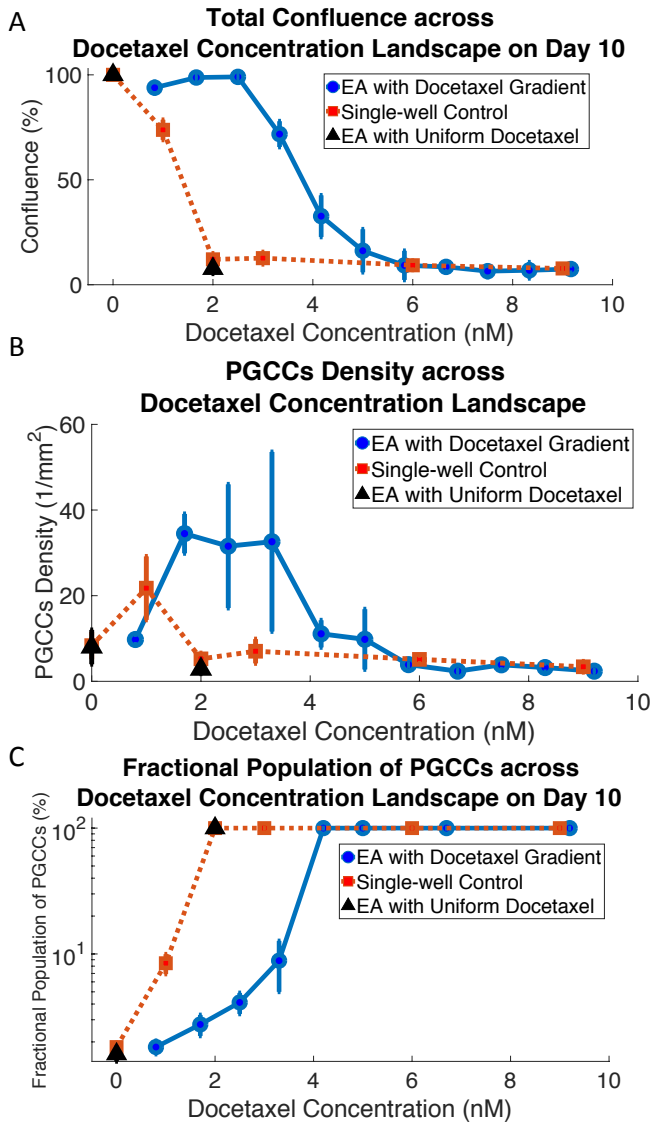


**Figure 4. Cell population versus docetaxel concentration on day 10.** (A) Total confluence. Compared with single-well control, in the EA with docetaxel gradient there were far more cells at higher docetaxel levels from 2 nM to 4 nM. (B) The density of PGCCs. Within the range of 2 nM to 4 nM docetaxel, the density of PGCCs increased by a large factor in the EA when with a drug gradient in comparison with the control conditions. (C) The fractional population of PGCCs. Within the region where PGCC density greatly increased, the fractional population of PGCCs was very low (10% or less), meaning there were an extremely large number of diploid cells. The coexistence of PGCCs and diploid cells could be correlated with elevated PGCC emergence. Under all scenarios, PGCCs were the only survivors at 4 nM and above.

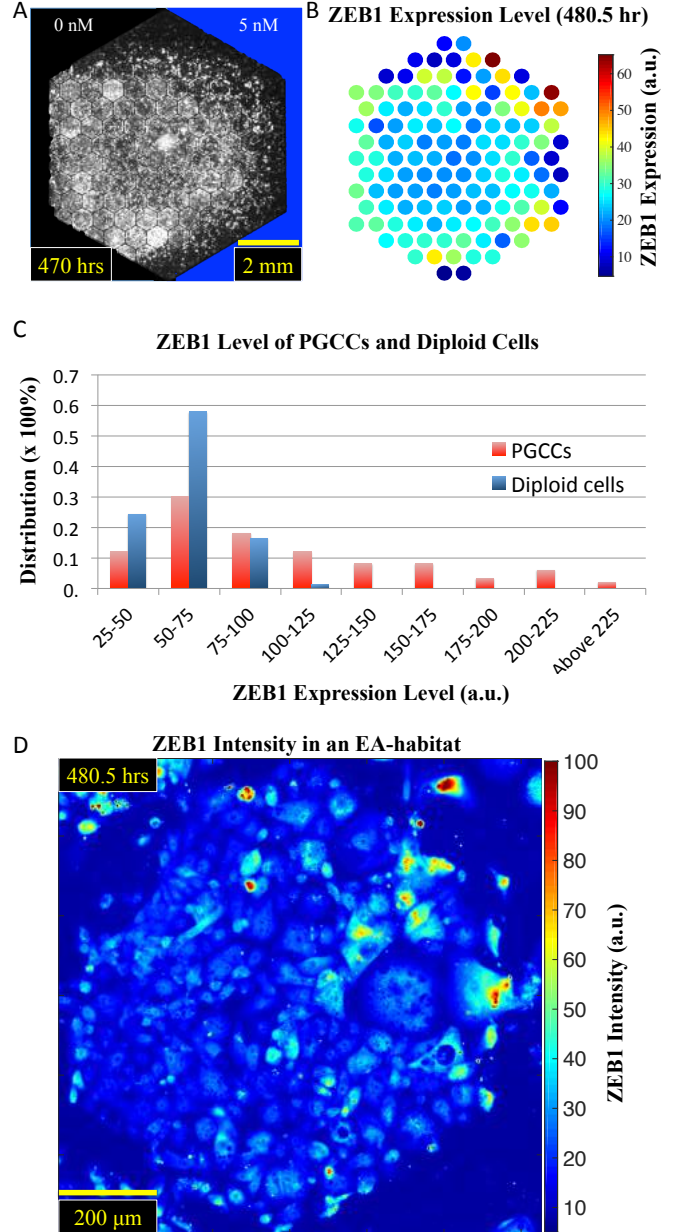


**Figure 5. ZEB1 expression level of PC3-Epi after being cultured in docetaxel gradient, from 0 to 5 nM, for 20 days.** (A) The mCherry fluorescent image of the entire EA. (B) The heat-map of ZEB1 expression level across the device. Each dot represents the average ZEB1 level of cells in the corresponding EA. (C) The normalized histogram of ZEB1 level of PGCCs and diploid PC3-Epi cells showing the significant elevation of ZEB1 expression in PGCCs. (D) The color-mapped ZEB1 intensity in one EA element where PGCCs coexisted with diploid PC3-Epi cells. PGCCs stain more positively than diploid cells.

The number of PGCCs per unit area was vastly enriched and more PGCCs resided in region with higher dosage of docetaxel (Fig. 4 (B)), revealing the importance of a gradient in PGCC emergence. Within the range of 2 nM to 4 nM docetaxel, the density of PGCCs increased by a remarkably large factor (from  $\sim 4$   $1/mm^2$  to  $\sim 35$   $1/mm^2$ , nearly 10X) in the EA when with a drug gradient in comparison with both control conditions (the conventional single wells and the EA with uniform drug concentration).

For the control experiment, the fractional population of PGCCs without chemotherapeutic stress is 2%. At 1 nM, the fraction of PGCCs increased to 9%. Above 2 nM, the population was exclusively composed of PGCCs. In contrast, the fraction of PGCCs of the EA gradient experiment is significantly lower within the range of 1-3 nM docetaxel, which implies the coexistence of a large number of diploid cells ( $>300$   $1/mm^2$ ) and PGCCs at 1-3 nM docetaxel. In contrast, in a conventional well plate, almost no diploid cells at all survived after 10 days in 2 nM docetaxel.

In order to verify that the difference in population dynamics between the EA gradient experiment and the single-well control experiment is not due to technical artifacts associated with our cell culture platform, we performed a set of control experiments in the EA with uniform docetaxel dosage, 0 nM and 2 nM. As shown in Fig. 4, the result was in accordance with the single-well controls. Therefore, the phenomena of increased survival of PC3-Epi population under high dosage are indeed the result of the heterogeneous environment (the stress gradient).

## 2.2 Characterization of PGCCs emergence: polyploidization mechanism and ZEB1 expression

The large cells at the highest docetaxel concentrations had very distinct morphologies. The cell diameter had increased by an order of magnitude, from the ordinary 10 - 15  $\mu m$  to 100 - 200  $\mu m$ . Real-time single-cell characterization of nuclear dynamics was performed by simultaneous two-channel imaging of PC3-Epi cells co-expressing cytoplasmic mCherry protein and H2B-GFP labeled histones. Supplementary Figure 1 shows some examples of the heterogeneity of the mechanisms by which the original diploid PC3-Epi cells became PGCC cells including both failed cytokinesis and cell fusion. A video of these complex dynamics in one microhabitat can be found in the Supplementary Material, H2B-GFP-EPI.avi. The soft-condensed matter aspects of these dramatic cell fusion events is a subject that needs to be pursued [20].

Most chemotherapeutic agents have been reported to induce EMT in the vast majority of solid cancers[21, 22, 23]. As a first step towards probing the hypothesis that the emergence of PGCCs is a critical process in metastasis via the EMT process, we cultured PC3-Epi in the EA with a docetaxel gradient (from 0 to 5 nM) for 20 days, as shown in Fig. 5 (A). IF analysis was performed subsequently to further characterize the expression level of ZEB1, a mesenchymal biomarker that is associated with cancer invasiveness and metastasis.

PC3-Epi is an established monomorphic cell sub-line without mesenchymal characteristics. After being exposed to docetaxel gradient for 20 days, there was a significant elevation of ZEB1 expression in the population, as shown in Fig. 5 (B). Each dot represents the average ZEB1 level of cells in the corresponding microhabitat. The expression level increased significantly around and beyond the lethal high cytotoxicity boundary, similar to the PGCC distribution pattern demonstrated in Fig. 2.

The normalized histogram Fig. 5 (C) shows that the ZEB1 level of PGCCs was increased compared with diploid cells. As shown in Fig. 5 (D) where PGCCs coexisted with diploid cells, most PGCCs stained more positively than diploid cells. The fact that PGCCs have statistically significant mesenchymal biomarker expression compared with the diploid cells suggests that the PGCCs are equipped with greater phenotypic plasticity, conferring a superior adaptation potential in order to survive stressful environment. Our data show a great deal of heterogeneity within our EA, as would be expected in a tumor.

## 2.3 Quantification of cancer population dynamics and cell migration

To identify the underlying mechanism of the increased polyploidization events in docetaxel gradient, it is necessary to quantify key parameters which regulate population dynamics. Here we modified the well-known logistic growth equation applied to both diploid and polyploidy cells by introducing the polyploid transformation term. We can fit the equation to data from single-well control experiments to determine the parameters. We also tracked cell motion and quantified the migration events that occurred in the EA with docetaxel gradient. The acquired parameters would then be used to describe cancer population dynamics with and without cell migration factors as discussed in the Discussion section, revealing the fundamental role of cells migration over a stress gradient in tumor development.

First, we assume that the cancer population is composed of 2 interchangeable phenotypes, the diploid cancer cells ( $u$ ) and the PGCCs ( $v$ ). The cancer population is broken up into 11 subpopulations in a linear microhabitat array. Each subpopulation  $i$  is locally homogeneous and connected to the adjacent subpopulations  $i - 1$  and  $i + 1$ . A docetaxel gradient (0 to 10 nM) is stably established across the microhabitat array so that the local docetaxel concentration within each subpopulation is  $C_i = i - 1$  (nM). The local population dynamics of diploid cells ( $u_i$ ) and PGCCs ( $v_i$ ) in the subpopulation  $i$  can be described using a set of non-linear differential equations based on the logistic growth equation,

$$\begin{aligned} \frac{du_i}{dt} &= u_i(G_i - k_u(u_i + v_i) - T_i) + M_{im,i} - M_{em,i}, \\ \frac{dv_i}{dt} &= u_i T_i - v_i(k_v(u_i + v_i) - D_i), \end{aligned} \quad (1)$$

where the docetaxel concentration dependent parameters  $G_i$ ,

$T_i$  and  $D_i$  are proliferation rate of diploid cells, transformation rate from diploid to PGCCs, and death rate of PGCCs, respectively. The transformation from PGCCs to diploid progeny was not observed within the time frame of the experiment and is therefore absent in the equation.  $k_u$  and  $k_v$  are the cell capacity limiting constants of diploid cells and PGCCs, which are independent of the dosage of docetaxel.  $u(G_i - k_u(u + v))$  is considered the density-dependent effective proliferation rate of diploid cells, while  $uT_i - k_v v(u + v)$  is considered the effective PGCC emergence rate.  $M_{im,i}$  and  $M_{em,i}$  are the amount of cell migration into / out of subpopulation  $i$ . Although PGCCs have been observed to be extremely deformable and can migrate through the slits, the migration probability is very low compared with diploid cells. Therefore we assume the migration of PGCCs to be zero. The mechanism of chemotherapy-induced diploid cell death is generalized as a 2-step process, mitotic arrest followed by delayed mitosis-linked cell death. Therefore, the drug induced diploid cell death is included in transformation term  $u_i T_i$  and PGCC death term  $v_i D_i$ .

The aforementioned parameters  $G_i$ ,  $T_i$ ,  $D_i$ ,  $k_u$  and  $k_v$  can be obtained by fitting the equations to single-well control data of diploid and PGCCs as a function of time in different docetaxel concentration, as listed in table 1 in the Supplementary Material. The migration terms were ignored in the single-well control experiment where no migration occurred. The total cell number as a function of time and the fractional population of PGCCs measured in single-well control experiments were fitted using the weighted least-squares method. As shown in Supplementary Figure 2 (A), the equation describes the population progression reasonably well.

The migration factor is determined by cell tracking measurement of the EA experiment with docetaxel gradient (0 - 10 nM). As shown in Supplementary Figure 2 (B), the cell emigration events in each microhabitat is roughly linearly correlated to the cell number within the microhabitat in a period of 45 hours. In addition, there is no dependency between drug concentration and emigration/cell count ratio. If they are alive, they migrate independent of drug concentration. Finally, there is no observable tendency for diploid cells to migrate toward higher or lower drug concentration. Their migration is random. Therefore, the emigration and immigration terms  $M_{em}$  and  $M_{im}$  can be described as

$$\begin{aligned} M_{em,i} &= \mu u_i, \\ M_{im,i} &= \frac{1}{2}(M_{em,i-1} + M_{em,i+1}) = \frac{\mu}{2}(u_{i-1} + u_{i+1}), \end{aligned} \quad (2)$$

The slope of the regression line in Supplementary Figure 2 (B) is about 0.9, which means the migration probability  $\mu$  for each cell is  $\approx 0.9/45 = 0.02$  (1/hr).

### 3. Discussion

The presented population study demonstrated that the gradient stress environment generated a population that could survive

at stress levels that could not be achieved when the environment had no gradient. When a stable docetaxel gradient was applied in the EA for 10 days, we observed a cytotoxic transition between fully confluent zone and the PGCC-dominant zone. Compared with the control experiment, the lethal high cytotoxicity boundary shifted from 2 nM to 6 nM, and the density of PGCCs was enriched in region with higher dosage of docetaxel.

The underlying mechanism of the aforementioned observation is studied using mathematical model described in equation (1). The model demonstrated that the coexistence of proliferative and resistant phenotypes with the ability to migrate across a spatially-varying stress landscape could lead to significant improvement of survival of cancer cells. With the parameters in equation (1) quantified based on single-well experimental data, the population dynamics of the both single-well control and EA experiment with docetaxel gradient can be reconstructed without introducing any other free parameters, as demonstrated in Fig. 6 (A) (B). The only difference between the modeled single-well control and modeled EA experiment is the migration factor. Compared with experimental result presented in Fig. 4 (A) (C), the modeling results share similar features. The total cell confluence shifted about 2 nM, and the density of PGCCs increased dramatically within the similar range of docetaxel concentration. To be clear, equation (1) does not include other potential mechanisms such as niche construction in densely populated domain or the diffusion of cell signaling molecules which may confer an advantage to cells in adjacent regions.

The basic reasoning for the observed population dynamics can be grasped from a game theory analogy [24], as shown in Fig. 7 (A). In a conventional cell culture plate, when the cells are exposed to chemotherapy above a certain dosage, the cells will either become polyploid or more likely apoptotic. The maximum number of PGCCs would be pre-determined by the initial diploid density, since diploid proliferation would be limited. Consider the case when the cancer cells are exposed to a stress gradient. In the high drug concentration region the cells die but a portion of the population become polyploid in response to the chemotherapy, but with low numbers and slow to zero growth rates. In the meantime, the population in the low drug concentration region is dominated by the highly-proliferative diploid phenotype that continues to proliferate. Most significantly, this large number of diploids can now migrate into higher drug regions, acting as generators of PGCCs. Therefore, unlike the conventional cell culture plate, the population in the high stress zone is replenished by cell migration and thus the number of PGCCs is not limited by the initial size of population in the high drug region. This qualitative explanation is supported by our quantitative model as demonstrated in Fig. 7 (B) (C). The diffusive migration of diploid cells creates a positive cell influx from low to high drug concentration (Fig. 7 (B)). The accumulated cell influx, which consists of proliferative diploid cells, leads to higher diploid population in region with higher docetaxel concen-



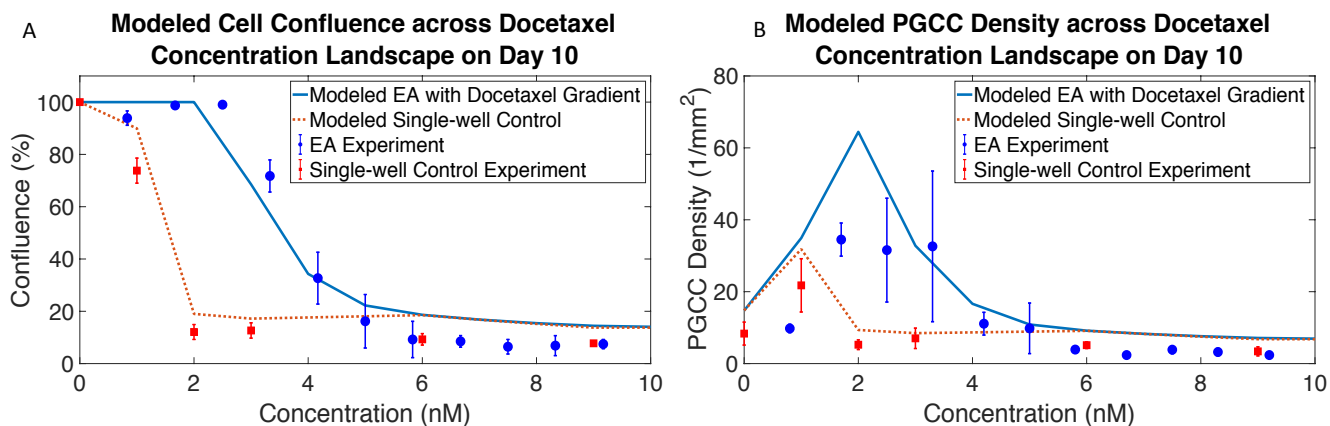


**Figure 6. The modeling of cancer population as a function of docetaxel concentration on day 10.** (A) Total cell confluence versus docetaxel concentration. (B) Density of PGCCs versus docetaxel concentration. The modeling of both cell confluence shifting and PGCC abundance are in accordance with the features of experimental results.

tration. The migrated diploid cells then rapidly transform to PGCCs, because the transformation rate is increased by the stress from the drug. As a result, many more PGCCs are formed in a gradient environment than in uniform drug environments.

To emphasize how and where PGCCs are produced in the EA, the effective PGCC emergence rate can be calculated by multiplying local diploid population  $u_i$  and transformation rate  $T_i$  and subsequently subtracting the population capacity limiting term  $v_i k_v (u_i + v_i)$ , as shown in Fig. 7 (C). The modeling result shows that the random migration of diploid cells is sufficient to give rise to an elevated PGCC emergence observed in experiment.

Realistic biological environments typically have population and drug gradients of many different values, so the basic phenomena must be explored over many values simultaneously. In this paper, we have demonstrated that the observed increased survival of the cancer population and the enrichment of PGCCs in the chemotherapeutic stress environment is facilitated by a gradient in stress levels. We have also demonstrated with our microfluidic EA that the emergent PGCCs have significant up-regulation of mesenchymal biomarker ZEB1 compared with the diploid cells, implying that PGCCs were more capable of exploring the phenotypic landscape and finding better survival and metastatic strategies. The mechanism of how PGCCs become resistant is beyond the scope of this paper. Instead, the highlight of this work is that what appears to be a rare event in homogeneous environments can be amplified in a stress gradient. Our observation provides an insight into the development of drug resistance in a tumor tissue: when more tumorigenic and highly-evolvable polyploid cell subpopulations are generated during the treatment due to the environmental heterogeneity, it is more likely that the tumor becomes resistant.

It has been reported that the technology based on semi-isolated populations in a gradient environment accelerates the evolutionary dynamics to take place over weeks in the

lab rather than months in conventional static culture *in vitro* assays [16, 25, 26]. For instance, Wu *et al.* demonstrated that the degree of doxorubicin resistance of multiple myeloma increased 16-fold after 48 hrs of doxorubicin gradient exposure [25], and Lin *et al.* presented the microfluidic system which allows the observation of on-chip docetaxel resistance development and relapse of prostate cancer PC3 in 2 weeks [16]. However, there has been no satisfactory explanation for how the rapid evolution is achieved. Our results and the game theory analogy could also provide microscopic evidence for the underlying mechanism: the continuous production of PGCCs which possess high phenotypic plasticity and chromosomal instability.

There is in addition a strong resemblance between the polyploidization response of cancer cells to chemotherapy resulting in increased fitness and the emergence of multinucleated bacterial [27] when *E. coli* are treated with the genotoxic antibiotic ciprofloxacin. Multi-chromosome-containing bacteria are able to divide asymmetrically at sub-lethal concentrations of ciprofloxacin and produce progeny with increased resistance. The mechanism of bacterial filament formation is analogous to the generation of PGCCs, which suggests a unified fundamental role of polyploidy emergence in conferring resistance.

We note that it has been extensively demonstrated that cell dynamics within tumor microenvironment can be a crucial factor in tumor progression, drug resistance development, and cancer metastasis. [28, 29] For instance, stromal cells have been demonstrated to suppress the apoptosis signal of cancer cells, mediate *de novo* drug resistance, [30] and contribute to CCR5-dependent promotion of metastatic tumor growth. [31] Immune cells are also known to promote epithelial-mesenchymal transition (EMT) and generate cancer stem cells within the cancer ecosystem. [32, 33] These intercellular dynamics are typically difficult to study *in vitro* in the context of environmental heterogeneity. Although not presented in this paper, our current work includes co-cultures



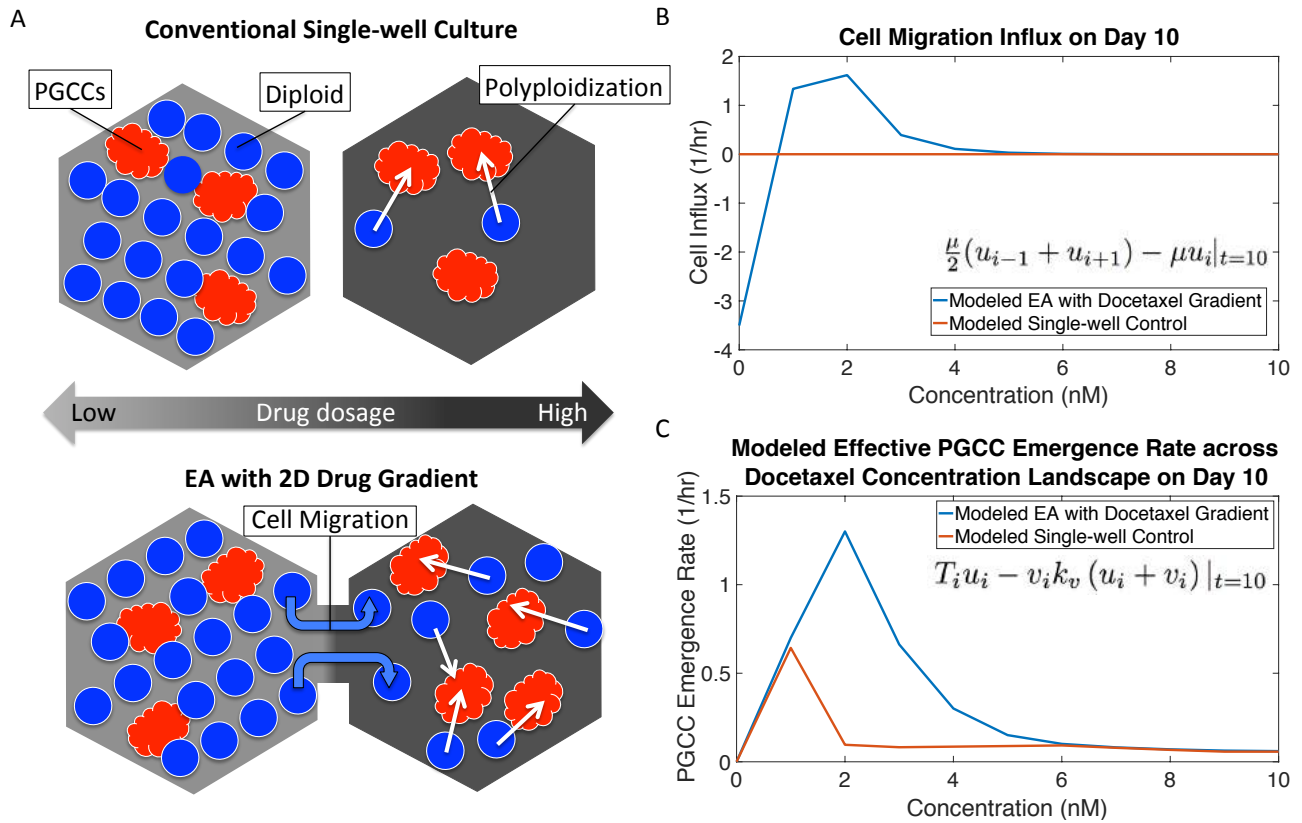


**Figure 7. Explanation of elevated PGCC emergence in chemotherapy gradient as opposed to a well-mixed environment.** (A) Schematic figure of the game theory analogy. In conventional culture, cells with drug dosage reach high confluence and the fraction of PGCCs remains low. The cells in high dosage well either undergo apoptosis or polyploidization, leaving only the PGCCs in the culture. In the EA gradient experiment, on the other hand, the populations under different level of stress are interconnected. The diploid cells continue to proliferate in EA areas with low drug, and can migrate to high drug EA areas, providing new source of PGCCs but at a high risk of death. (B) Diploid cell migration influx as a function of docetaxel concentration on day 10. Diploid cells are constantly supplied into higher docetaxel concentration region. (C) The effective PGCC emergence rate defined as  $T_i u_i$  subtracted by population capacity limiting term  $v_i k_v (u_i + v_i)$ . By simply allowing cell migration, the effective PGCC emergence rate can be greatly affected.

of cancer and stromal cells in an effort to address these issues.

Using a heterogeneous environment typical of a real biological system has allowed us to see how the mixture of normal diploid cells and the PGCCs can result in better fitness to high levels of a therapy such as docetaxel. This suggests the clinical value of identifying vulnerabilities of PGCCs might be targeted as critical targets [34]. Ideally, we should be able to identify some vulnerabilities of PGCCs that even diploid cancer cells generically do not have, in a way that would not trigger a stress response in the diploid cancer cell tumor population, which unfortunately usually leads to increased resistance. An important therapeutic implication of our findings is that inhibiting centrosome clustering might well retard the development of drug resistance in tumors. Inhibiting centrosome clustering would be a promising therapeutic target because it would be likely prevent an effective response to a stressful drug.

## 4. Methods

### Cell lines and reagent

The human prostate cancer line PC3, originally established from a patient with bone metastasis, was obtained from the American Type Culture Collection (ATCC, Manassas, VA). PC3-Epi and PC3-EMT cells were generated in the Pienta lab as previously described by Roca *et al.* [18]. PC3-Epi is an E-cadherin/CDH1-positive/vimentin-negative PC3 clone and PC3-EMT is a mesenchymal derivative that has an E-cadherin-negative/vimentin-positive phenotype.

All the cells are cultured in RPMI 1640 (Gibco, Grand Island, NY) supplemented with 10% fetal bovine serum (Sigma-Aldrich, St. Louise, MI) and 1X Anti-anti (Gibco, Grand Island, NY). To generate chemotherapy gradient, desired dosage of docetaxel (Selleck Chemical LLC, Houston, TX) was dissolved in RPMI media and filled into syringes, tubings and reservoirs of the device.

### Fabrication of the PDMS device

The design and setup of the system are based on our previous publication. [16] As shown in Supplementary Figure 3 (A), the tri-layered PDMS device consists of a reservoir layer, a capping layer and a micro-engineered PDMS EA pattern, bonded together by oxygen plasma treatment. The reservoir layer was designed to trap air bubbles from the tubings. The PDMS EA pattern is fabricated by standard lithography techniques. A silicon wafer was patterned by photolithography and deep reactive-ion etching for 100  $\mu\text{m}$ , followed by silanization for PDMS molding. Sylgard<sup>®</sup> 184 silicone elastomer kit was mixed and poured onto the silanized silicon mold, degassed and cured at 70 °C overnight. The PDMS chip may later be peeled off from the mold, bonded with the reservoir and capping layer.

### Experiment setup

Supplementary Figure 3 (B) illustrates the components of our customized Lumox<sup>™</sup> plate holder. This customized holder is designed to provide thermal equilibrium condition, high relative humidity (above 90%) and ideal gas composition for cell growth. The gas channels allow gas inflow which pressurizes cell culture membrane on Lumox<sup>™</sup> plate and seals the chip.

A day before an experiment, the cells shall be seeded into the Lumox<sup>™</sup> plate with cell culture inserts, preferably exclusively in the region where the EA pattern is going to cover. At most six Lumox<sup>™</sup> plates can be held on the customized Lumox<sup>™</sup> plate holder. The PDMS device shall be sterilized by UV exposure and kept in aseptic environment.

To initiate the experiment, the PDMS device shall be connected to syringes via tubings. The syringes, tubings and the on-chip reservoirs are filled up media with reagent of interest and the PDMS pattern should be properly wetted. The chip is then placed directly on top of the Lumox<sup>™</sup> plate where the cells grow. After settling the devices, the gas supply system is then connected to the gas channels in the customized Lumox<sup>™</sup> plate holder, pressurizing the space between the Lumox<sup>™</sup> plate and the six wells, pushing the Lumox<sup>™</sup> membrane against the PDMS device to secure the sealing of the device.

The entire culture can be place on incubator microscope set around 37 °C and 5% CO<sub>2</sub> conditioned gas for long term time lapse scanning. After weeks of image acquisition, the chip can be removed and the cells can be fixed and sampled for further downstream analysis with immunofluorescence or DNA/RNA sequencing.

### Image Processing

The images presented in this paper were captured by Nikon TE2000 microscope with NIS-Elements imaging software. Images were converted into TIFF format for sequential image processing and measurement using Fiji. [35]

To categorize cells by size as demonstrated in Fig. 2, we created a custom image processing macro on Fiji based on the “rolling ball” algorithm ([https://imagej.net/Rolling\\_Ball\\_Background\\_Subtraction](https://imagej.net/Rolling_Ball_Background_Subtraction)) to enhance cell segmentation and improve the performance of Particle Analysis feature in Fiji ([https://imagej.net/Particle\\_Analysis](https://imagej.net/Particle_Analysis)). To begin with, we performed rolling ball algorithm on the original image with the rolling ball diameter set to be larger than that of the largest cell in the region of interest in order to remove coarse background variations. Sequentially, we performed rolling ball algorithm on the background-subtracted image with the rolling ball diameter lower than that of the smallest cell. This process is sensitive to intensity variations and therefore highlights the cell boundaries. Finally, we subtracted the boundary-highlighted image from the background-subtracted image to create a better-segmented image, which was then analyzed using Particle Analysis feature in Fiji for cell categorization by given diameter threshold.

## Disclosure of Potential Conflicts of Interest

The authors declare no potential conflicts of interest.

## Acknowledgements

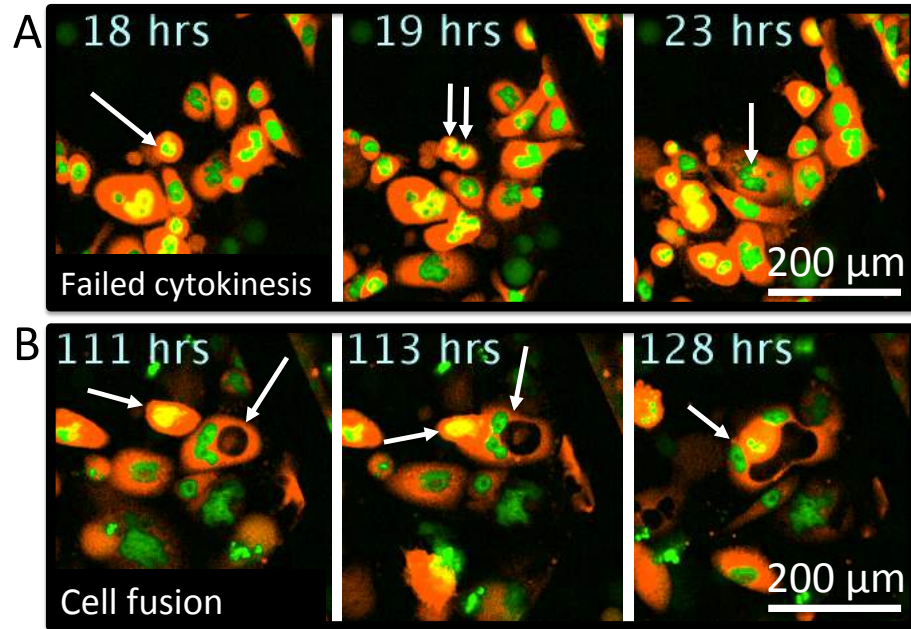
We would like to thank fruitful discussions with Dr. Yibin Kang. This work was supported by NSF PHY-1659940.

## References

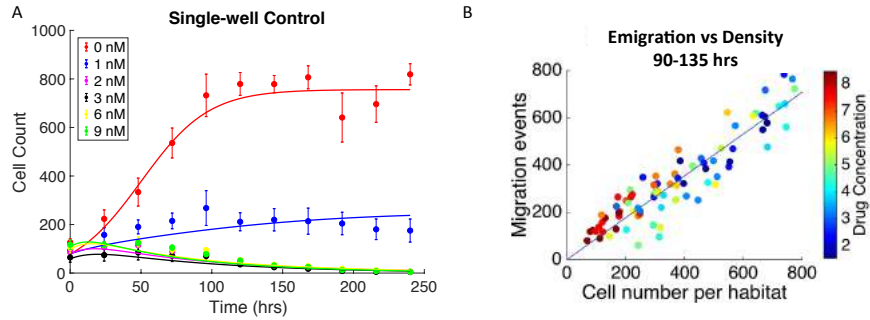
- [1] William H. Wolberg, W. Nick Street, and Olvi L. Mangasarian. Importance of nuclear morphology in breast cancer prognosis. *Clinical Cancer Research*, 5(11):3542–3548, 1999.
- [2] Karuna Mittal, Shashi Donthamsetty, Ramneet Kaur, Chunhua Yang, Meenakshi V Gupta, Michelle D Reid, Da Hoon Choi, Padmashree C G Rida, and Ritu Aneja. Multinucleated polyploidy drives resistance to Docetaxel chemotherapy in prostate cancer. *British Journal of Cancer*, 116(9):1186–1194, 2017.
- [3] Jekaterina Erenpreisa, Andrei Ivanov, Sally P Wheatley, Elizabeth A Kosmacek, Fiorenza Ianzini, Alim P. Anisimov, Michael Mackey, Paul J. Davis, Grigorijs Plakhins, and Timothy M. Illidge. Endopolyploidy in irradiated p53-deficient tumour cell lines: Persistence of cell division activity in giant cells expressing Aurora-B kinase. *Cell Biology International*, 32(9):1044–1056, 2008.
- [4] Antonia P Sagona and Harald Stenmark. Cytokinesis and cancer. *FEBS Letters*, 584(12):2652–2661, 2010.
- [5] Yuji Nakayama, Asae Igarashi, Ikue Kikuchi, Yuuki Obata, Yasunori Fukumoto, and Naoto Yamaguchi. Bleomycin-induced over-replication involves sustained inhibition of mitotic entry through the ATM/ATR pathway. *Experimental Cell Research*, 315(15):2515–2528, 2009.
- [6] Xin Lu and Yibin Kang. Cell fusion as a hidden force in tumor progression. *Cancer Research*, 69(22):8536–8539, 2009.
- [7] Xin Lu and Yibin Kang. Efficient acquisition of dual metastasis organotropism to bone and lung through stable spontaneous fusion between mda-mb-231 variants. *Proceedings of the National Academy of Sciences*, 106(23):9385–9390, 2009.
- [8] Timothy M Illidge, Mark S Cragg, Birgitta Fringes, Peggy Olive, and J a Erenpreisa. Polyploid giant cells provide a survival mechanism for p53 mutant cells after DNA damage. *Cell biology international*, 24(9):621–33, 2000.
- [9] A N Makarovskiy, E Siryaporn, D C Hixson, and W Ak-erley. Survival of docetaxel-resistant prostate cancer cells in vitro depends on phenotype alterations and continuity of drug exposure. *Cellular and Molecular Life Sciences*, 59(7):1198–1211, 2002.
- [10] Angela Ogden, Padmashree C G Rida, Beatrice S. Knudsen, Omer Kucuk, and Ritu Aneja. Docetaxel-induced polyploidization may underlie chemoresistance and disease relapse. *Cancer Letters*, 367(2):89–92, 2015.
- [11] Pierre Emmanuel Puig, Marie Noëlle Guilly, André Bouchot, Nathalie Droin, Dominique Cathelin, Florence Bouyer, Laure Favier, François Ghiringhelli, Guido Kroemer, Eric Solary, François Martin, and Bruno Chauffert. Tumor cells can escape DNA-damaging cisplatin through DNA endoreduplication and reversible polyploidy. *Cell Biology International*, 32(9):1031–1043, 2008.
- [12] Shiwu Zhang, Imelda Mercado-Uribe, Samir Hanash, and Jinsong Liu. ITRAQ-based proteomic analysis of polyploid giant cancer cells and budding progeny cells reveals several distinct pathways for ovarian cancer development. *PLoS ONE*, 8(11):1–16, 2013.
- [13] S Zhang, I Mercado-Uribe, Z Xing, B Sun, J Kuang, and J Liu. Generation of cancer stem-like cells through the formation of polyploid giant cancer cells. *Oncogene*, 33(1):116–28, 2014.
- [14] Laura M. Lopez-Sánchez, Carla Jimenez, Araceli Valverde, Vanessa Hernandez, Jon Peñarando, Antonio Martinez, Chary Lopez-Pedreira, Juan R. Muñoz-Castañeda, Juan R. De La Haba-Rodríguez, Enrique Aranda, and Antonio Rodriguez-Ariza. CoCl<sub>2</sub>, a mimic of hypoxia, induces formation of polyploid giant cells with stem characteristics in colon cancer. *PLoS ONE*, 9(6), 2014.
- [15] Z. Storchova and D. Pellman. From polyploidy to aneuploidy, genome instability and cancer. *Nat Rev Mol Cell Biol*, 5(1):45–54, 2004.
- [16] Ke-chih Lin, Gonzalo Torga, Amy Wu, Joshua D Rabinowitz, Wesley J Murray, James C Sturm, Kenneth J Pienta, and Robert Austin. Epithelial and mesenchymal prostate cancer cell population dynamics on a complex drug landscape. *Convergent Science Physical Oncology*, 3(4):045001, 2017.
- [17] Thomas Brabletz, Raghu Kalluri, M. Angela Nieto, and Robert A. Weinberg. Emt in cancer. *Nature Reviews Cancer*, 18:128 EP –, 01 2018.
- [18] Hernan Roca, James Hernandez, Savannah Weidner, Richard C. McEachin, David Fuller, Sudha Sud, Taibriana Schumann, John E. Wilkinson, Alexander Zaslavsky, Hangwen Li, Christopher A. Maher, Stephanie Daignault-Newton, Patrick N. Healy, and Kenneth J. Pienta. Transcription Factors OVOL1 and OVOL2 Induce the Mesenchymal to Epithelial Transition in Human Cancer. *PLoS ONE*, 8(10), 2013.
- [19] Teru Kanda, Kevin F. Sullivan, and Geoffrey M. Wahl. Histone-GFP fusion protein enables sensitive analysis of chromosome dynamics in living mammalian cells. *Current Biology*, 8(7):377–385, 1998.

- [20] F. Wottawah, S. Schinkinger, B. Lincoln, R. Ananthkrishnan, M. Romeyke, J. Guck, and J. Kas. Optical rheology of biological cells. *Phys Rev Lett*, 94(9):098103, 2005.
- [21] Haixia Long, Tong Xiang, Wei Qi, Jiani Huang, Junying Chen, and Luhang He. cancer cell metastasis via CCL5 induced epithelial-mesenchymal transition. *Oncotarget*, 6(8):13–14, 2015.
- [22] Michele Cioffi, Crescenzo Dalterio, Rosalba Camerlingo, Virginia Tirino, Claudia Consales, Anna Riccio, Caterina Ierandò, Sabrina Chiara Cecere, Nunzia Simona Losito, Stefano Greggi, Sandro Pignata, Giuseppe Pirozzi, and Stefania Scala. Identification of a distinct population of CD133 + CXCR4 + cancer stem cells in ovarian cancer. *Scientific Reports*, 5:1–11, 2015.
- [23] Hyun Hee Lee, Vanessa Bellat, and Benedict Law. Chemotherapy induces adaptive drug resistance and metastatic potentials via phenotypic CXCR4-expressing cell state transition in ovarian cancer. *PLoS ONE*, 12(2):1–17, 2017.
- [24] R Axelrod and WD Hamilton. The evolution of cooperation. *Science*, 211(4489):1390–1396, 1981.
- [25] Amy Wu, Qiucen Zhang, Guillaume Lambert, Zayar Khin, Robert a. Gatenby, Hyunsung John Kim, Nader Pourmand, Kimberly Bussey, Paul C. W. Davies, James C. Sturm, and Robert H. Austin. Ancient hot and cold genes and chemotherapy resistance emergence. *Proceedings of the National Academy of Sciences*, 112(33):10467–10472, 2015.
- [26] Jeonghun Han, Yukyung Jun, So Hyun Kim, Hong-Hoa Hoang, Yeonjoo Jung, Suyeon Kim, Jaesang Kim, Robert H. Austin, Sanghyuk Lee, and Sungsu Park. Rapid emergence and mechanisms of resistance by U87 glioblastoma cells to doxorubicin in an in vitro tumor microfluidic ecology. *Proceedings of the National Academy of Sciences*, 113(50):14283–14288, 2016.
- [27] Julia Bos, Qiucen Zhang, Saurabh Vyawahare, Elizabeth Rogers, Susan M. Rosenberg, and Robert H. Austin. Emergence of antibiotic resistance from multinucleated bacterial filaments. *Proceedings of the National Academy of Sciences*, 112(1):178–183, 2015.
- [28] Mark B. Meads, Lori A. Hazlehurst, and William S. Dalton. The bone marrow microenvironment as a tumor sanctuary and contributor to drug resistance. *Clinical Cancer Research*, 14(9):2519–2526, 2008.
- [29] Kenneth H Shain and William S Dalton. Environmental-mediated drug resistance: a target for multiple myeloma therapy. *Expert Review of Hematology*, 2(6):649–662, 2009.
- [30] Yulia Nefedova, Pingyan Cheng, Melissa Alsina, William S. Dalton, and Dmitry I. Gabrilovich. Involvement of notch-1 signaling in bone marrow stroma-mediated de novo drug resistance of myeloma and other malignant lymphoid cell lines. *Blood*, 103(9):3503–3510, 2004.
- [31] Robert L Mango, Hendrik W van Deventer, Qing Ping Wu, and Jonathan S Serody. Pulmonary stromal cells expressing cc-chemokine receptor 5 promote metastasis via erythroid differentiation regulator 1. *Blood*, 114(22):3601–3601, 2009.
- [32] Jelani C Zarif, Russell S Taichman, and Kenneth J Pienta. Tam macrophages promote growth and metastasis within the cancer ecosystem. *OncImmunology*, 3(7):e941734, 2014. PMID: 25954596.
- [33] Jennifer M. Reiman, Keith L. Knutson, and Derek C. Radisky. Immune promotion of epithelial-mesenchymal transition and generation of breast cancer stem cells. *Cancer Research*, 70(8):3005–3008, 2010.
- [34] Jermaine Coward and Angus Harding. Size Does Matter: Why Polyploid Tumor Cells are Critical Drug Targets in the War on Cancer. *Frontiers in oncology*, 4(May):123, 2014.
- [35] Johannes Schindelin, Ignacio Arganda-Carreras, Erwin Frise, Verena Kaynig, Mark Longair, Tobias Pietzsch, Stephan Preibisch, Curtis Rueden, Stephan Saalfeld, Benjamin Schmid, Jean-Yves Tinevez, Daniel James White, Volker Hartenstein, Kevin Eliceiri, Pavel Tomancak, and Albert Cardona. Fiji: an open-source platform for biological-image analysis. *Nature Methods*, 9:676, jun 2012.





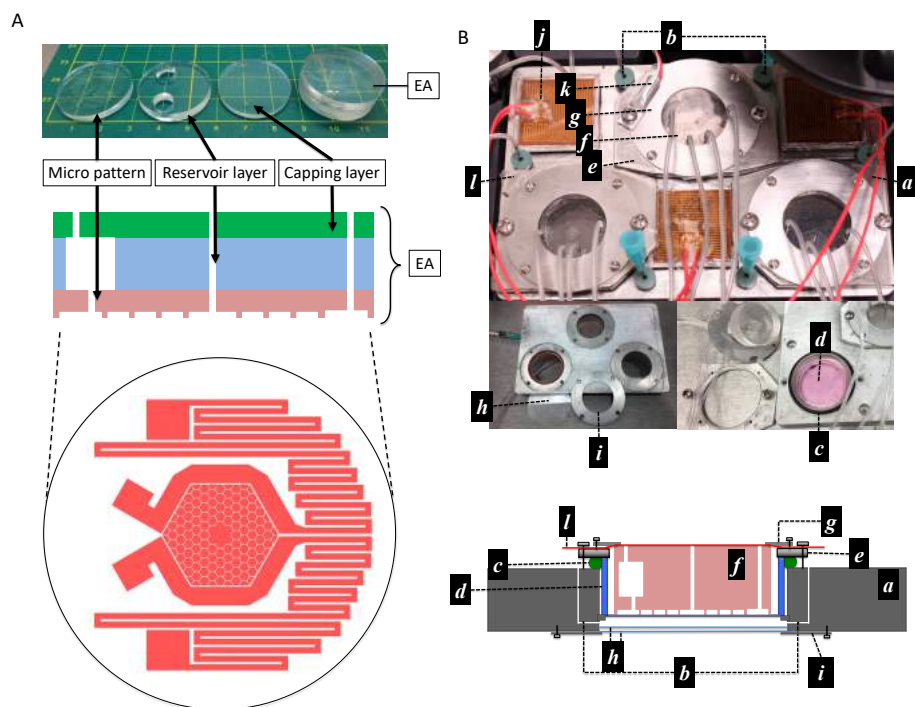
**Supplementary Figure 1. Different mechanism of polyploidization process of cancer cells in docetaxel gradient.** The mCherry-expressing PC3-EPI cell line was transfected with H2B-GFP plasmid to visualize chromatin. (A) Failed cytokinesis. A cancer cell at high dosage region attempted to divide but could not finish the mitosis process, ended up being polyploid. (B) Cell fusion. The two marked cells at high dosage region fused as one.



**Supplementary Figure 2. Parameters of the cancer population model described in equation (1) corresponded to experimental data.** (A) The growth curves of single-well control experiments fitted by equations (1) without migration terms. With 3 drug concentration dependent parameters ( $G$ ,  $T$ ,  $D$ ) and 2 drug concentration independent parameters ( $k_u$ ,  $k_v$ ), the progression of population can be described reasonably well. (B) Cell tracking analysis of EA experiments with docetaxel gradient (0 - 10 nM). The scatter plot shows the number of emigration events occurred within 45 hours versus the number of cells in each corresponding microhabitat. The data points are color-coded to present local docetaxel concentration. The slope of the linear regression line determines the probability of a cell leaving current habitat within 45 hours, which leads to the value of  $\mu$ , the migration probability as described in equations (2).

$C$ (nM)	$G$	$T$	D	$k_u$	$k_v$	$\mu$
0	0.047	0.0043	0	$4*5.7e-5$	$4*2.9e-4$	$4*0.02$
1	0.028	0.014	0.02			
2	0.038	0.05	0.02			
>3	0.037	0.05	0.02			

**Table 1.** The value of parameters used in the cancer population model.



**The experimental setup.** (A) The PDMS device. From left to right: the patterned layer, the reservoir layer, the capping layer, and the assembled device. The reservoirs trap bubbles in the tubing and secure stable fluidic dynamics. The serpentine channels allow the medium to equilibrate with the conditioned gas passed below the gas permeable Lumox<sup>TM</sup> membrane. (B) The components of the customized Lumox<sup>TM</sup> plate holder. *a*, the main body; *b*, gas channels that allow conditioned gas influx to pressurize Lumox<sup>TM</sup> membrane; *c*, an O-ring that seals the space between the well plate and the Lumox<sup>TM</sup> dish; *d*, the 35 mm Lumox<sup>TM</sup> dish; *e*, the dish holder; *f*, the PDMS device; *g*, the PDMS chip holders; *h*, the double layer 35 mm glass windows designed to maintain thermal isolation and prevent water condensation; *i*, glass window holder; *j*, heating pads; *k*, temperature sensor; *l*, the Microseal<sup>TM</sup> B Adhesive Sealer that keeps the chip from drying out. Images are adapted from “Epithelial and mesenchymal prostate cancer cell population dynamics on a complex drug landscape,” *Convergent Science Physical Oncology*, 3(4):045001, 2017.